

Charge Density of MgO: Implications of Precise New Measurements for Theory

J. M. Zuo,¹ M. O'Keeffe,² P. Rez,¹ and J. C. H. Spence¹

¹*Department of Physics and Astronomy, Arizona State University, Tempe, Arizona 85287*

²*Department of Chemistry, Arizona State University, Tempe, Arizona 85287*

(Received 27 January 1997)

A tenfold improvement in the accuracy of measured low-order structure factors for MgO has been achieved using the convergent beam electron diffraction technique. These results allow a meaningful comparison to be made with the latest calculations. We find that the MgO charge density can be described by a superposition of spherical Mg^{2+} and O^{2-} ions, but that a small nonspherical distortion of Mg and O is observable in both experiment and theory. The experimental charge distribution of O^{2-} is more diffuse than the theory, which may be due to the breathing effect of O^{2-} in a vibrating lattice. [S0031-9007(97)03416-9]

PACS numbers: 61.14.-x, 61.50.Lt, 71.20.-b

Our knowledge of crystal bonding is often derived from indirect evidence and theory rather than from the direct measurement of charge densities. An example is NaCl, which is the prototype of ionic bonding. Yet, the experimental evidence for ionicity cited in textbooks (e.g., [1]) has an uncertainty in the measured structure factors (SF) [2] far larger than the difference between models consisting of neutral atoms or ions [3]. The most accurately known experimental charge density is for silicon [4]. The availability of large, perfect grown silicon crystals makes it possible to apply the Pendelösung method which takes full account of multiple scattering effects. However, ionic crystal charge densities are not as well known. The accuracy of x-ray and γ -ray SF measurements [5,6] is limited by extinction effects to about 1%. For strong reflections, such as the (200) of MgO, measurement errors in previous experiments greatly exceed differences calculated for different bonding models.

We have developed a versatile and general quantitative convergent beam electron diffraction (CBED) technique for accurate measurement of structure factor amplitudes and phases [7]. The method takes advantage of the sub-nanometer probe available in the field emission electron microscope. Using such a small probe, a region of perfect crystal can almost always be found. The small-angle scattering of high energy electrons also significantly reduces the influence of residual strains from defects. We compare the experimental intensity profile across a CBED disk (the rocking curve) with calculations. The theoretical intensity is calculated using the Bloch wave method [8], with structure factors, absorption coefficients, the beam direction, and thickness as refinable parameters. Electron diffraction measures the Fourier coefficients of the Coulomb potential directly; these are related to the charge density through Poisson's equation. A small change in the low-order x-ray structure factors leads to a large relative change in the Fourier coefficients of the potential. Thus electron diffraction measurements are extremely accurate for low-order "bonding" structure factors. Tests

with silicon show that the structure factors of both strong and weak reflections can be measured with an accuracy level of about 5 me/atom, comparable to the best x-ray Pendelösung measurements [9].

MgO low-order structure factors up to (422) were measured by the CBED method at room temperature. Seven separate measurements were made for different reflections. Five of these measurements were done on the same MgO platelet. Estimated errors [10] for the important (111) and (200) reflections are a factor of 10 smaller than for previous x-ray measurements [11]. Details of the measurement are given in a separate paper [10]. The structure factors for (511) and higher were taken from the single-crystal x-ray measurements of Lawrence [12]. These are important for the determination of Debye-Waller factors. Lawrence's measurements are chosen over similar measurements by Sanger [11] because Sanger's MgO crystal was intentionally damaged by neutron irradiation to reduce extinction effects. Lawrence and Sanger's data differ systematically for the weak odd-order reflections. Table I lists our room temperature (RT) structure factor measurements up to (400). For comparison, various theoretical models are also listed. The theoretical RT structure factors listed are calculated using Debye-Waller factors of $B_{\text{Mg}} = 0.305(2)$ and $B_{\text{O}} = 0.340(3)$, with $B_{\text{av}} = 0.319 \text{ \AA}^2$, which are obtained from model analysis of the measured structure factors (see below). The crystal structure factor was calculated using the full-potential linearized augmented plan wave method (LAPW) using the WIEN95 package [13]. Both the local density approximation (LDA) [14] and generalized gradient approximation (GGA) [15] were used. The GGA goes beyond the LDA by including the first derivative of electron density in the exchange and correlation energy functional. Parameters such as the muffin-tin (MT) radius and number of k points were varied to ensure numerical convergence. Following the example of Lu *et al.* [16], we assigned individual temperature factors for charges inside each muffin-tin sphere and an averaged Debye-Waller factor for charges between the MT spheres.

TABLE I. Listing of the present measured low order structure factors of MgO, and comparison with theory.

<i>hkl</i>	Present	DF-N ^a	DF-ION ^b	LDA ^c	GGA ^d
111	11.142(20)	12.389	11.090	11.175	11.082
200	52.89(3)	52.030	53.040	52.765	52.918
220	40.68(8)	41.073	41.062	40.953	41.072
311	12.41(12)	12.309	12.633	12.356	12.401
222	33.75(12)	34.005	33.800	33.777	33.865
400	29.01(8)	28.993	28.790	28.949	29.012
...
<i>R</i> factor		0.011	0.0072	0.0063	0.0067

^aSuperimposed spherical atoms.

^bIons calculated using the Dirac-Fock method.

^cCrystal structure factor calculated using LAPW and LDA.

^dCrystal structure factor calculated using LAPW and GGA.

The atomic charge densities were calculated using the multiconfigurational Dirac-Fock (MCDF) program [17]. The O²⁻ ion was stabilized using the Watson +2 potential well [18]. Table I shows *R* factors comparing theory and the SF data set of the present measurements, together with the high-order structure factors of [12]. The lowest *R* factor was obtained using the LAPW and the LDA. For the O²⁻ Watson model, a 1.2 Å sphere radius fit best.

Figure 1 shows a map of the difference between the crystal charge density and that of superimposed neutral atoms for a (100) plane of the cubic unit cell of MgO, for both experiment and theory (LAPW using LDA). For the theoretical map, atomic references were calculated using LDA. The experimental map was obtained using the multipole fitting data described below. Both experiment and theory clearly indicate charge transfer from Mg to O, although strictly speaking it is not possible to define charge transfer uniquely from the static charge density [19]. The theoretical charge density can be directly compared with models, and this favors a description with a charge transfer of two [20,21]. Experimentally, the

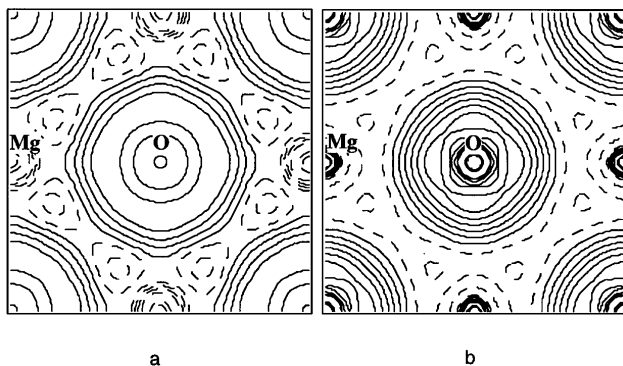


FIG. 1. The (001) plane difference charge density map between crystal and superposition of neutral atoms for (a) experiment and (b) LAPW using LDA. For details, see text. O sits at the corner and the center of the map, while Mg is at the middle of the edge. The contour interval is 0.03 e/Å³.

direct measurement of charge density is limited to a few SF's. Here we propose a particularly useful scheme for distinguishing different bonding models by using the scattering factor of the transferred electrons Δf . For MgO, Δf is defined as the difference between the crystal SF and that for Mg²⁺O, calculated using a spherical Mg²⁺ ion and a neutral oxygen:

$$\Delta f = (-1)^{h+k+l}[F(h,k,l) - 4f^{\text{Mg}^{2+}}(s) - (-1)^{h+k+l}4f^{\text{O}}(s)]/4. \quad (1)$$

The phase factor $(-1)^{h+k+l}$ is applied because, in the ionic model, the two Mg 3s electrons are transferred to oxygen, which is displaced by a vector $(\frac{1}{2}, \frac{1}{2}, \frac{1}{2})$ relative to Mg. In the neutral-atom model, the 3s electron wave function is centered on the Mg site, and Δf will fluctuate due to the phase factor, whereas, in the fully ionic model, Δf should follow the smooth curve given by the difference between the scattering factors of O²⁻ and O, or $f_{2p} = f_{\text{O}^{2-}} - f_{\text{O}}$. Figure 2 plots Δf for the experimental and LAPW structure factors and f_{2p} , obtained using the Dirac-Fock method and a Watson sphere of 1.2 Å radius. The largest contribution comes from (111) and (200). It is clear that overall both the experimental and theoretical Δf resemble f_{2p} . A model of Mg²⁺O⁻ with the remaining electron distributed more or less uniformly for the charge density of MgO was proposed by Vidal-Valat *et al.* [22] and Bukowinsky [23]. For this model, Δf is about half f_{2p} since the remaining uniformly distributed electron only contributes at the origin. This model does not give a good description of the experimental results.

There are systematic differences between the charge densities of the experiment, the LAPW-LDA, and the spherical Mg²⁺O²⁻ model, as shown in Fig. 1. The experimental charge density has a much lower minimum than the theory. Figure 1 also shows clear deviations in both experiment and the LAPW-LDA structure factors from the smooth curve of the spherical ion model; this

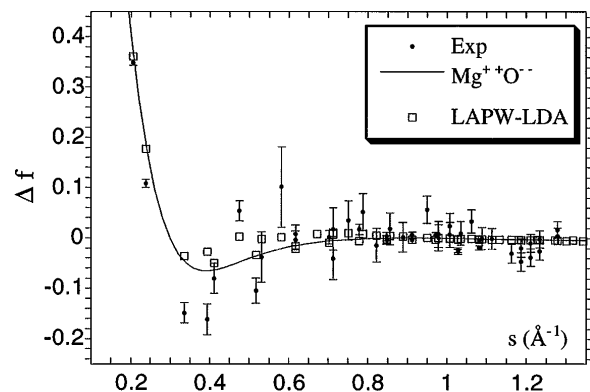


FIG. 2. Scattering factor (Δf) of the two Mg 3s electrons at an oxygen site obtained from experiment, the LAPW using LDA, and the Watson sphere model.

suggests a nonspherical charge distribution. To quantify these differences, following the example of Dawson [24], Stewart [25], and Coppens *et al.* [26], we propose the following charge density model:

$$F(h, k, l) = 4(f'_{\text{Mg}^{2+}} + (2 - q)f_{3s} + \delta f^1) \times \exp(-B_{\text{Mg}}s^2) + 4(-1)^{h+k+l} \times (f'_O + qf_{2p} + \delta f^2)\exp(-B_Os^2). \quad (2)$$

Here, scaled spherical Mg^{2+} and O charge densities are used as a reference, and f is the atomic scattering factor. The scaling is carried out using $f' = \sum_n f_n(s/\kappa_n)$, with scaling constant κ_n . For the deeply bound $1s$ electrons, the influence of crystal fields is generally small, so that $\kappa_n = 1$. Ionic bonding is described by introducing the charge transfer q . Here f_{3s} is the scattering factor of the Mg $3s$ electrons, and f_{2p} is the difference scattering factor between O^{2-} and O. To a good approximation, we found that f_{2p} is well described by the Fourier transform of the function $r^{n-2}e^{-\alpha r}$. Here n and α are determined by fitting. For O^{2-} , calculated using a Watson sphere, $n = 5$ fits best. The δf terms in Eq. (2) describe the contribution of the centrosymmetric nonspherical term in the crystal charge density. We consider only the $l = 4$ Kubic harmonic term (the lowest nonzero term). The associated charge density in real space is

$$\rho(\mathbf{r}) = 13.68534HN_h r^n \exp(-\beta r) \times [(x^4 + y^4 + z^4)/r^4 - 3/5] \quad (3)$$

with $N_h = \beta^{n+3}/(n+2)!$, and H and β are determined by fitting. Table II summarizes the results of the fitting for both the experimental and calculated LAPW charge density using LDA. The parameters were gradually introduced into the refinement to check the significance of each parameter. For the experiment, the refined Debye-Waller factors for Mg and O are almost independent of the model. The averaged Debye-Waller factor is 0.319 \AA^2 , slightly larger than $0.308(3)$ obtained from thermodynamic measurement [27]. Both the experimental and theoretical charge density are well described by the spherical-ion model, with scaling. For the experimental charge density, we found that it is only necessary to scale the $2p$ electrons in Mg and O. For the LAPW charge density, scaling of the $2s$ electrons is also important

due to the additional charge modulation in the core region in the LAPW charge densities. The introduction of nonspherical terms in the model only improves the R factor by 0.03% and 0.02% for the experimental and theoretical charge densities. Both experimental and theoretical charge densities are well described by the full ionic model with a charge transfer of two electrons. Both experiment and theory indicate the existence of hexadecapole modulations. However, the magnitude of the nonspherical term is difficult to quantify due to the limitations of experimental accuracy and the proposed charge density model. The effect of the hexadecapole term is opposite for Mg and O. For oxygen the charge is slightly distorted towards the Mg^{2+} , and for Mg^{2+} the charge is pushed away from O^{2-} . The biggest difference between LAPW-LDA and experiment (Fig. 3) is the distribution of the extra two electrons near O. Figure 3 plots the spherically averaged charge density difference between O^{2-} and O as found from the model refinements for both experiment and LAPW-LDA. For comparison, the Watson model of O^{2-} is also plotted. The size of O^{2-} in the Watson model increases with the radius of the potential well. As seen in Fig. 3, the experimental charge is significantly moved outwards, indicating a bigger and more diffuse O^{2-} ion in the real crystal. This difference is due largely to the (200), (220), and (311) structure factors, which consistently show a lower Δf than theories (Fig. 1). The difference is significantly larger than the estimated experimental error in those reflections. This difference in oxygen charge distribution, which is significantly larger than the difference between theories, could be due to the failure of the rigid ion approximation, or the polarizability of O^{2-} . Presumably, the charge distribution of O^{2-} is given by the average of the instantaneous charge configurations determined by vibrating neighboring ions, rather than the static one assumed in the theoretical calculations. The change of O^{2-} charge distribution with lattice potential is known as the breathing effect.

A larger O^{2-} ion is also consistent with the measured mean potential (Φ_O) of MgO, which is $13.01(8) \text{ V}$ [28]. According to Bethe [29], the mean potential of an atom is proportional to $\langle r^2 \rangle$, and so is highly sensitive to atomic expansion, and can be calculated from the pseudoatoms of the multipole model. The best-fit parameters of Table II give $\Phi_O = 12.76 \text{ V}$ for experiment and 12.28 V for the

TABLE II. Results of model fitting of experimental and theoretical charge density of MgO. The scaling constant κ_n is listed for $1s$ and $2p$.

	$(\kappa_n - 1)\%$	Mg β	H	B	$(\kappa_n - 1)\%$	O β	H	α	B	$q(e)$	$R \times 10^{-3}$
Expt.	0; 0.26			0.306	0; 1.2			9.04	0.340		6.46
$m = 9, n = 6$	0; 0.17	4.62	0.30	0.306	0; 0.4	3.88	-0.11	7.95	0.339	2.0	6.12
LDA	0.15; -0.3				1.3; 0.26			6.17			0.84
$m = 6, n = 5$	0.15; -0.3	6.27	0.19		1.4; 0.3	3.62	-0.14	6.06		2.0	0.67

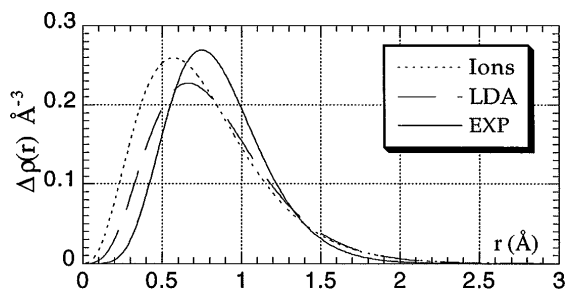


FIG. 3. Spherical averaged charge-density difference between O^{2-} and O for experiment, the LAPW (LDA), and the Watson sphere model (ions).

LAPW charge density, using LDA. A crystal consisting of spherical Mg^{2+} and O^{2-} ions calculated using MCDF and a 1.2 Å Watson sphere radius has $\Phi_O = 12.18$ V. For the mean potential of MgO, the contributions of Mg^{2+} and O are about 17% and 42%, respectively, and they change little from one theoretical model to another. The main difference between the calculated Φ_O is the difference between charge density of O^{2-} and O . If we assume $\Delta\rho(r) \propto r^{n-2}e^{-\alpha r}$ for these two electrons in a real crystal and $\langle r^2 \rangle$ values for Mg^{2+} and O from the MCDF calculations, we obtain $\alpha = 7.84$ from the measured Φ_O , which is in excellent agreement with the multipole model value.

In conclusion, low-order structure factors of MgO are accurately determined, and used to test theories. Good agreement with the measured experimental structure factors was obtained using the LAPW method, the LDA or GGA exchange and correlation potential, and the Dirac-Fock spherical O^{2-} ion calculated using a Watson sphere of 1.2 Å. Both the experimental and the LAPW theoretical charge densities are well approximated by a superposition of spherical Mg^{2+} and O^{2-} ions. The systematic difference between the measured experimental structure factors and theories indicates a more diffusive distribution of O^{2-} charge density than that predicted by LAPW or the Dirac-Fock O^{2-} ion. Deviations of the experimental and LAPW structure factors from the spherical ion model suggest a nonspherical distortion. Inclusion of a hexadecapole term in the charge density model improves the R factor by 0.002 to 0.003 for both theory (LAPW) and experiment. This indicates that nonspherical charge distortion is small in the ionic bonding of MgO. These findings were made possible using accurately measured low-order structure factors obtained by electron diffraction, especially for the (111), (200), and (220) reflections.

This work is supported by awards NSF9412146 and CRDF RP1-208.

- [1] C. Kittel, *Solid State Physics* (Wiley, New York, 1986).
- [2] G. Schoknecht, *Z. Naturforsch.* **12**, 983 (1957).
- [3] G. Böbel, P. Cortona, and F. G. Fumi, *Acta Crystallogr. A* **45**, 112 (1989).
- [4] S. Cumming and M. Hart, *Aust. J. Phys.* **41**, 423 (1988).
- [5] C. J. Howard and R. D. G. Jones, *Acta Crystallogr. A* **33**, 776 (1977).
- [6] M. C. Schmidt, R. Collella, and D. R. Yoder-Short, *Acta Crystallogr. A* **41**, 171 (1985).
- [7] J. M. Zuo and J. C. H. Spence, *Ultramicroscopy* **35**, 185 (1991); J. M. Zuo, *Acta Crystallogr. A* **49**, 429–435 (1993).
- [8] J. C. H. Spence and J. M. Zuo, *Electron Microdiffraction* (Plenum, New York, 1992).
- [9] M. Saunders *et al.*, *Ultramicroscopy* **60**, 311 (1995); G. Ren, J. M. Zuo, and L. M. Peng, *Micron* (to be published).
- [10] J. M. Zuo (to be published).
- [11] P. L. Sanger, *Acta Crystallogr. A* **25**, 694 (1969).
- [12] J. L. Lawrence, *Acta Crystallogr. A* **29**, 94 (1973).
- [13] P. Blaha, K. Schwarz, P. Dufek, and R. Augustyn, WIEN 95, Technical University of Vienna 1995. [Improved and updated unix version of the original copyrighted WIEN-code published by P. Blaha, K. Schwarz, P. Sorantin, and S. B. Trickey in *Comput. Phys. Commun.* **59**, 399 (1990)].
- [14] J. P. Perdew and Y. Wang, *Phys. Rev. B* **45**, 13 244 (1992).
- [15] J. P. Perdew, J. A. Chevary, S. H. Vosko, K. A. Jackson, M. R. Pederson, D. J. Singh, and C. Fiolhais, *Phys. Rev. B* **46**, 6671 (1992).
- [16] Z. W. Lu and A. Zunger, *Acta Crystallogr. A* **48**, 545 (1992).
- [17] I. P. Grant, B. J. McKenzie, P. H. Norrington, D. F. Mayers, and N. C. Pyper, *Comput. Phys. Commun.* **21**, 207 (1980).
- [18] R. E. Watson, *Phys. Rev.* **111**, 1108 (1958).
- [19] C. R. A. Catlow and A. M. Stoneham, *J. Phys. C* **16**, 4321 (1983).
- [20] J. Redinger and K. Schwarz, *Z. Phys. B* **40**, 269 (1981).
- [21] M. J. Mehl, R. E. Cohen, and H. Krakauer, *J. Geophys. Res.* **93**, 8009 (1988).
- [22] G. Vidal-Valat, J. P. Vidal, and K. Kurki-Suonio, *Acta Crystallogr. A* **34**, 594 (1978).
- [23] M. S. T. Bukowski, *J. Geophys. Res.* **85**, 285 (1980).
- [24] B. Dawson, *Acta Crystallogr. A* **25**, 12 (1969).
- [25] R. F. Stewart, *J. Chem. Phys.* **58**, 1668 (1973).
- [26] P. Coppens, T. N. Guru Row, P. Leung, E. D. Stevens, P. J. Becker, and Y. W. Yang, *Acta Crystallogr. A* **35**, 63 (1979).
- [27] T. H. K. Barron, *Acta Crystallogr. A* **33**, 602 (1977).
- [28] M. Gajdardziska-Josifovska *et al.*, *Ultramicroscopy* **50**, 285 (1993).
- [29] M. O'Keefe and J. C. H. Spence, *Acta Crystallogr. A* **50**, 33 (1994).